Understanding the heavy fermion behavior in $CeInPt_4$

A. D. Hillier, D. T. Adroja, S. R. Giblin, and W. Kockelmann
ISIS Facility, Rutherford Appleton Laboratory, Chilton, Oxfordshire OX11 0QX, United Kingdom

B. D. Rainford
Department of Physics and Astronomy, University of Southampton, Southampton SO17 1BJ, United Kingdom

S. K. Malik
International Center for Condensed Matter Physics (ICCMP), University of Brasilia, 70904-970 Brasilia, Distrito Federal, Brazil
(Received 16 May 2007; revised manuscript received 6 September 2007; published 30 November 2007)

The cubic compound $CeInPt_4$ exhibits heavy fermion behavior with a high extrapolated value of the electronic specific heat, $\gamma=2.5$ J/mole K^2 as $T\rightarrow 0$ K. The specific heat does not exhibit any sign of long range magnetic ordering down to 100 mK. In order to understand the origin of the high value of γ and the nature of the $4f$ electrons of this compound, we have carried out neutron diffraction, low-field magnetic susceptibility, muon spin relaxation, and inelastic neutron scattering measurements on $CeInPt_4$. Our susceptibility results show that for temperatures between 20 and 1.5 K, a power law behavior is exhibited, $\chi(T)\sim T^{-\beta}$ with $\beta=0.5$. Below 1.5 K, the susceptibility is almost temperature independent, again without any sign of magnetic ordering down to the lowest available temperature (300 mK). The muon spin relaxation measurements reveal that below 1 K, the electronic relaxation rate strongly increases without any loss of muon initial asymmetry, indicating the presence of low energy spin fluctuations as an explanation for the high value of γ in $CeInPt_4$. Heat capacity data reveal a $\log(C/T)\propto\log(T)$ behavior, indicating that $CeInPt_4$ may exhibit non-Fermi-liquid behavior close to a $T\rightarrow 0$ K quantum critical point. Our inelastic neutron scattering results reveal a broad crystal field excitation centered at 25 meV, indicating the presence of strong hybridization between the $4f$ and the conduction electrons, which is consistent with the observed high value of the paramagnetic Curie temperature ($\theta_p=-255$ K).

DOI: 10.1103/PhysRevB.76.174439 PACS number(s): 71.10.Hf, 71.27.+a, 75.20.Hr

I. INTRODUCTION

Cerium based intermetallic compounds have generated considerable interest in the field of strongly correlated electron systems due to the observation of various novel ground state properties, such as heavy Fermion behavior, valence fluctuations phenomenon, coherent Kondo lattice effect, unconventional superconductivity, quantum criticality, and non-Fermi-liquid behavior.[1,2] Theoretical calculations based on Anderson's model indicate that many of these properties can be explained by considering the presence of strong hybridization between the localized $4f$ electrons and conduction electrons.[3,4] In the absence of hybridization, Ce compounds exhibit conventional magnetic ordering at low temperatures or remain paramagnetic, while with increasing strength of hybridization, the magnetic ordering temperature T_C passes through a maximum. Also, some Ce compounds have a similar value of T_C when compared to their isostructural Gd compounds,[5,6] which cannot be explained using de Gennes scaling. Further increasing the hybridization strength leads to novel ground states being observed, such as quantum criticality, and mixed valence or itinerant behavior for the strongest hybridization limit.[1,2]

Recently, RXT_4 (R=rare earths, X=In, Mn, and T=transition metals) compounds have attracted attention due to the interesting physical properties they exhibit, for example, a first order valence phase transition in $YbInCu_4$,[7] heavy Fermion behavior of $CeInPt_4$,[8,9] geometrical frustration in $RInCu_4$ compounds,[10] a Kondo-type rise in the resistivity of nonmagnetic $YInCu_4$,[11] and the prediction of Mn rattling modes in $CeMnNi_4$.[12] All these compounds crystallize in the ordered version of a $MgSnCu_4$ type structure, space group $F\bar{4}3m$ (No. 216).[13] Among these compounds, $CeInPt_4$ exhibits some fascinating behavior. Its electronic coefficient of heat capacity γ increases continuously with decreasing temperature and reaches 2.5 J/mole K^2 as $T\rightarrow 0$ K (extrapolated value). The origin of this high value of γ was not explained in the previous study.[9] In order to understand the high γ value in $CeInPt_4$, we have investigated the spin dynamics of $CeInPt_4$ using muon spin relaxation (μSR) measurements. Furthermore, we have carefully characterized the sample using powder neutron diffraction, magnetic susceptibility, and inelastic neutron scattering measurements.

Our μSR study reveals the presence of low energy spin fluctuations below 1 K. The μSR results along with $\log(C/T)\propto\log(T)$ behavior of the heat capacity indicate that the origin of the high value of γ in $CeInPt_4$ is due to non-Fermi-liquid (NFL) behavior arising from the quantum fluctuations at the $T=0$ phase transition. The neutron diffraction study reveals an ordered $MgSnCu_4$-type structure without any disorder between the In and Pt atoms and a high value of the thermal parameter for the In atoms. This indicates the presence of rattling modes for the In atoms. Further, the inelastic neutron scattering shows a broad crystal field excitation at 25 meV, indicating the presence of strong hybridization between $4f$ and conduction electrons.

II. EXPERIMENTAL DETAILS

A polycrystalline sample of $CeInPt_4$ was prepared in a water cooled copper hearth argon arc furnace using stoichiometric amounts of the constituent elements with a minimum purity of 99.9%. The ingot was melted and turned several times to ensure sample homogeneity. The weight losses during melting were negligible. The sample was powdered for the various experiments. Neutron powder diffraction, muon spin relaxation (μSR), and high energy inelastic neutron scattering measurements were carried out at the ISIS pulsed neutron and muon facility. The neutron diffraction study was carried out using the GEM diffractometer in order to determine the structure of $CeInPt_4$. The sample was filled into a cylindrical vanadium can, which gives a low coherent Bragg scattering. The data were analyzed with the GSAS program using all histograms of the six GEM detector banks. The low-field and low temperature susceptibility (below 2 K) measurements were performed using a homebuilt super conducting quantum interference device (SQUID) susceptometer at Durham University[14] (in an applied field of 10 μT), and high temperature (2–300 K) susceptibility measurements were carried out using a Quantum Design SQUID MPMS XL system (in an applied field of 10 mT). The heat capacity data were taken from Ref. 9, and the experimental details are given therein. The μSR experiments were carried out using the μSR spectrometer in longitudinal geometry. At the ISIS facility, a pulse of muons is produced every 20 ms and has a full width at half maximum of ~70 ns. These muons are implanted into the sample and decay with a half-life of 2.2 μs into a positron, which is emitted preferentially in the direction of the muon spin axis. These positrons are detected and time stamped in the detectors which are positioned before (F) and after (B) the sample. The positron counts $N_{F,B}(t)$ have the functional form

$$N_{F,B}(t) = N_{F,B}(0)\exp\left(-\frac{t}{\tau_\mu}\right)[1 \pm G_Z(t)], \quad (1)$$

where $G_z(t)$ is the longitudinal relaxation function. $G_z(t)$ is determined using

$$G_z(t) = \frac{N_F(t) - \alpha N_B(t)}{N_F(t) + \alpha N_B(t)}, \quad (2)$$

where α is a calibration constant which was determined at 4 K by applying a small transverse field (~20 G) and adjusting its value until the resulting damped cosine signal was oscillating around zero. This calibration constant takes into account detector efficiency and the absorption of positrons in the sample and surrounding equipment. The powdered sample was mounted onto a 99.995(+)% pure silver plate and was mixed with GE varnish in order to improve the thermal contact. This formed a thin disk which was 30 mm in diameter and 1 mm thick. Any muons stopped in silver gives a time independent background. The sample holder and sample were mounted onto a TBT dilution fridge with a temperature range of 45 mK to 4 K. The sample was then cooled down to base temperature in zero field (ZFC) and the μSR spectra were collected, firstly, upon warming the sample while still in zero field and, secondly, after ZFC and warming in a longitudinal field of 50 G. The inelastic neutron scattering measurements were carried out on the HET time of flight spectrometer at ISIS with an incident energy of 60 meV and at 13 K.

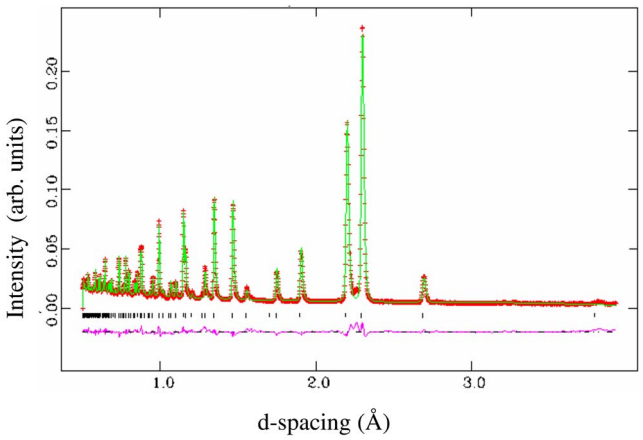

FIG. 1. (Color online) Rietveld fitted neutron diffraction pattern of $CeInPt_4$ at 300 K. The vertical tick marks indicate the calculated peak positions, and the lower graph shows the difference plot.

III. NEUTRON DIFFRACTION STUDY

Figure 1 shows a neutron diffraction pattern collected at 300 K on one of the six GEM detector banks.

The structure of $CeInPt_4$ can be derived from the cubic $AuBe_5$-type structure by replacing Au by Ce and selectively replacing two Be sites 4*c* and 16*e* by In and Pt atoms, respectively. This gives the ordered version of the $MgCuSn_4$-type structure for $CeInPt_4$ (see Fig. 2) compared with the disordered version of the $AuBe_5$-type structure in which one can assume statistical disorder between Pt and In

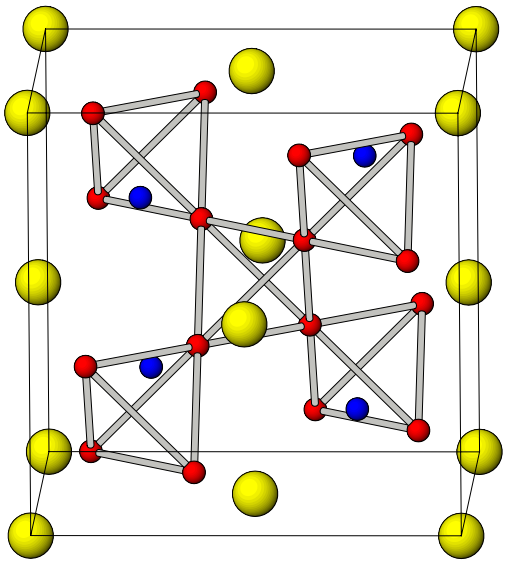

FIG. 2. (Color online) The crystal structure of $CeInPt_4$. The yellow atoms are Ce (large atoms), the blue atoms are In (small dark atoms), and the red atoms are Pt (small lighter atoms).

TABLE I. Refined parameters for $CeInPt_4$ at 300 K using the ordered model. The lattice parameter, a, is 7.6129(6) Å. The R_{wp} factor is 7.5%.

	x	y	z	Occupancy	$100U_{iso}$ (Å^2)
Ce	0.0	0.0	0.0	1.0 (fixed)	0.58(1)
In	0.25	0.25	0.25	0.97(3)	3.43(14)
Pt	0.625	0.625	0.625	0.90(1)	0.83(1)

occupancy on both crystallographic sites. To check the degree of ordering of In and Pt on two Be sites, Rietveld refinements were carried out using space group $F\bar{4}3m$ (No. 216) in which In and Pt occupy crystallographic inequivalent sites. It is to be noted that even though the $F\bar{4}3m$ space group has a possibility of ordered and disordered structures, there are no extra superlattice reflections present due to ordering. Ce is considered to occupy the crystallographic $4a$ (0, 0, 0) site, whereas for an ordered model, In and Pt atoms occupy exclusively the $4c$ $(\frac{1}{4},\frac{1}{4},\frac{1}{4})$ and the $16e$ (x,x,x) sites, respectively.

Refinements allowing In and Pt on both sites (disordered model) rely on the scattering contrast of the elements, which is given by the neutron scattering lengths of In (b=4.065-0.0539i fm) and Pt (b=9.6 fm). The analysis shows that the sample is of nearly single phase, with an unknown impurity which is less than 1%. For the analysis of the ordered structure model, we varied the lattice parameter, positional parameters for Pt, thermal parameters, and absorption parameters while keeping the site occupancies fixed, giving a good fit with a weighted profile R value of R_w=7.6%. In the second stage of the analysis, we varied the site occupancy of In and Pt while leaving the Ce fixed at full occupancy. This marginally improved the fit with R_w=7.5%, yielding In and Pt occupancies of approximately 1.0 and 0.9, respectively (see Table I). It should be noted that the fits were not significantly improved when exchange of In on the Pt site and Pt on the In site was permitted, yielding a small degree of disorder of about 7% In on the Pt site and vice versa, Pt on the In site (R_w=7.5%) Refined crystallographic parameters for the ordered model are given in Table I. It is interesting to note that the thermal parameter of In on $4c$ sites is almost an order of magnitude larger than the thermal parameter of Ce on the $4a$ site and Pt on $16e$ site. A similarly large value of the thermal parameter has been observed for rare earth atoms in the skutterudite's compound RT_4Sb_{12},[15] which has been attributed to the rattling modes of the rare earth atoms in a large void space available in the cubic structure of these compounds. It is interesting to compare the crystal structure results for $CeInPt_4$ and rattling modes in Mn substituted hexagonal $CeNi_5$, giving an ordered $CeMnNi_4$ alloy, also crystallizing in the $MgCuSn_4$-type structure.[13] A similarly ordered cubic structure has also been observed in the $UPdCu_4$ compound, which has attracted considerable interest in the field of non-Fermi-liquid studies.[16] Furthermore, it has been shown that the $MgCuSn_4$-type $CeMnNi_4$ is peculiar in that the Mn ions are enclosed in a large cage. Interestingly, the

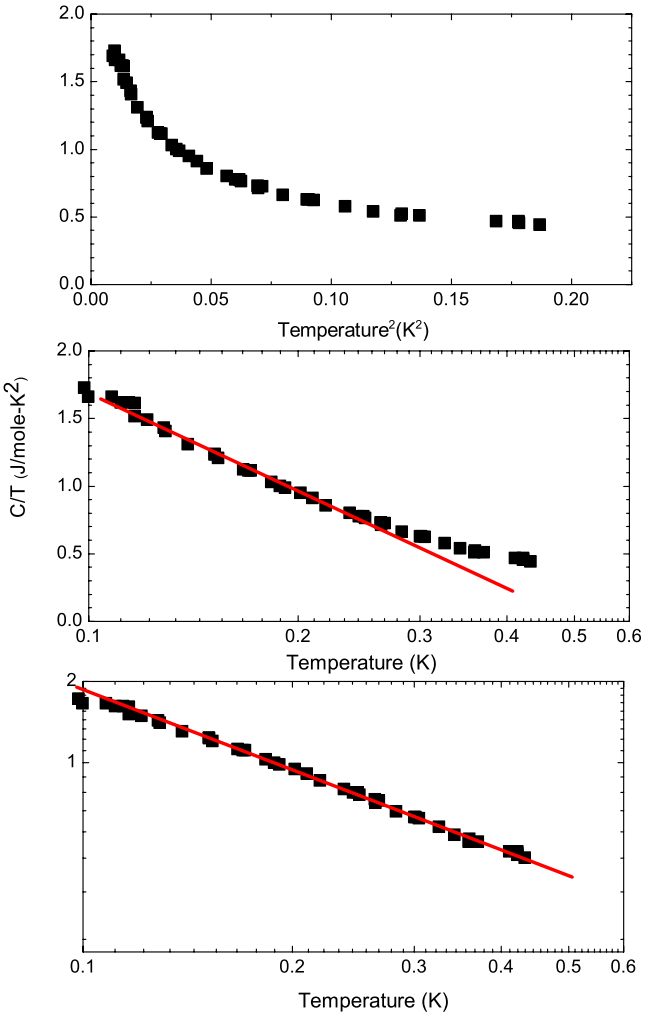

FIG. 3. (Color online) The upper graph shows the squared temperature dependence of C/T, the middle graph shows the logarithmic-linear relation of C/T at low temperatures, and the lower graph shows the log-log behavior for $CeInPt_4$.

low frequency rattling phonon modes have been theoretically predicted to occur in this compound.[12] Thus, we attribute the observed high value of the thermal parameter of the In atom in $CeInPt_4$, occupying the same site as Mn in $CeMnNi_4$, to rattling modes of the In atoms. If the x value of the Pt atoms comes close to a special position (5/8 5/8 5/8), then the lengths of Ce-Pt and In-Pt bonds become close. Our analysis gives interatomic distances of 3.1561(5) Å for Ce-Pt and 3.1562(5) Å for In-Pt, which are in agreement with the refined value of the x(Pt) parameter.

IV. HEAT CAPACITY AND MAGNETIC SUSCEPTIBILITY

Figure 3 (top) shows the heat capacity (C) measurements, from Ref. 9 plotted as C/T vs T^2. We have replotted these data as C/T vs log(T) in Fig. 3 (middle). It is clear that at low temperature (T), the heat capacity exhibits a logarithmic rise. This behavior of the heat capacity is very similar to that observed in non-Fermi-liquid systems, such as CeRhBi,[17]

$CeNi_9Ge_4$,[18] and $CeRh_{1-x}Pd_x$.[19] When the data are plotted as $\log(C/T)$ vs $\log T$ [Fig. 3 (bottom)], the power law behavior of the form $T^{-1+\epsilon}$ fits over the entire temperature range with a $\epsilon=0.04$. A similar power law behavior in the heat capacity of $Ce_{1-x}Th_xRhSb$ has been reported, (with $\epsilon=0.45$), which also exhibits non-Fermi-liquid behavior.[1] This behavior of the heat capacity of $Ce_{1-x}Th_xRhSb$ has been attributed to the disordered induced Griffiths cluster model. However, for $CeInPt_4$, ϵ is small compared to that for $Ce_{1-x}Th_xRhSb$. This difference of ϵ along with the ordered crystal structure suggests that the disorder is playing a minor role in $CeInPt_4$. It is worth noting that the value of γ obtained from plotting C/T vs T^2 is 2.5 J/mole K^2 when extrapolated to $T=0$.

Our present analysis indicates that the high value of γ of $CeInPt_4$ is due to NFL behavior arising due to the close proximity of a $T=0$ quantum critical point. It is interesting to note that the parent compound $CePt_5$, which crystallized in the hexagonal $CaCu_5$-type structure, orders antiferromagnetically with $T_N=1$ K, with a γ value of 30 mJ/mole K^2 at 0.2 K.[20] In $CeTPt_4$ where T=Ga or Al, which have the same crystal structure as $CePt_5$, a weakening of the magnetic interactions has been observed.[21,22] This supports our conjecture that magnetic ordering temperature of $CeInPt_4$ has been suppressed to $T\rightarrow 0$ K, which results in the enhancement of γ. Furthermore, according to single-ion Kondo theory, the Kondo temperature (T_K) is related to the maximum value of γ by the relation $T_K=0.68R/\gamma$, where R is the gas constant. This gives $T_K=2.2$ K when using $\gamma=2.5$ J/mole K^2 for $CeInPt_4$. Again, the estimated low value of T_K is in agreement with non-Fermi-liquid behavior close to a quantum critical point. At a local quantum critical point, one expects that both T_K and T_N approach 0 K.[23–26]

In order to further understand the ground state properties of $CeInPt_4$, we have measured the temperature dependence of the susceptibility, and the results are plotted in Fig. 4. For temperatures between 10 and 1.5 K, the magnetic susceptibility exhibits a logarithmic behavior. On reducing the temperature still further, the susceptibility is found to be weakly temperature dependent. These susceptibility results along with the heat capacity data of $CeInPt_4$ show some similarity to that observed in $CeNi_9Ge_4$, in which heat capacity exhibits a logarithmic rise, but susceptibility is almost constant at low temperatures.[18] This behavior has been attributed to an unusual non-Fermi-liquid behavior in $CeNi_9Ge_4$. Further, the high temperature susceptibility of $CeInPt_4$ exhibits Curie-Weiss behavior between 300 and 100 K with an effective moment of 2.54 μ_B and paramagnetic Curie temperature θ_p $=-225$ K [see Fig. 4 (bottom)]. The high value of θ_p indicates the presence of strong Kondo-type interactions and also a high value of the Kondo temperature T_K^H. Considering the single-ion Kondo model, $\gamma\propto 1/T_K^H$, this means that a high value of T_K^H will give a low value of γ, which is not the case for $CeInPt_4$. This supports the idea that the high value of γ for $CeInPt_4$ is due to this system exhibiting NFL behavior close to a quantum critical point. The origin of the high value of θ_p could be due to the crystal field and Kondo effect coming from the excited crystal field levels. For all the $RInCu_4$ compounds, the negative θ_p is significantly larger than the Néel temperature, indicating the presence of frustration.[10] The frustration parameter f, which is defined as

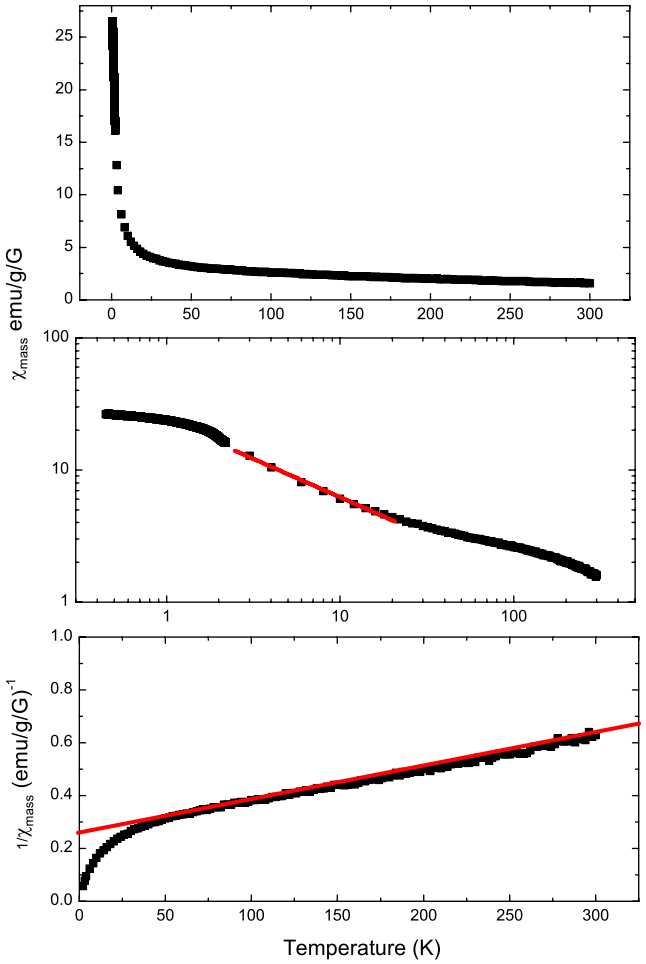

FIG. 4. (Color online) Temperature dependence of the magnetic susceptibility of $CeInPt_4$. The upper graph shows the high temperature Curie-Weiss behavior on a linear scale, whereas the middle graph shows the log-log temperature dependence of the magnetic susceptibility, which shows the weak temperature dependence at low temperatures and the linear behavior in the susceptibility, $\chi \sim aT^{-\beta}$, with $a=0.018$ and $\beta=0.5$. The lower graph shows inverse susceptibility

$f=\theta_p/T_N$, in general rarely exceeds 10. In the case of $RInCu_4$, the f value is 11.8 for Dy, 14.3 for Ho, and 12.6 for Er, and therefore, it has been concluded that frustration affects substantially the magnetic properties of these materials and also that θ_p and T_N obey de Gennes scaling.[10] This indicates that the observed frustration is a single-ion effect. As $CeInPt_4$ and $RInCu_4$ are isostructural, there is a possibility that a contribution to θ_p in $CeInPt_4$ may also come from the frustration effect as seen in $RCuIn_4$.

It is interesting to note that most of the heavy fermion systems exhibit a Wilson ratio of ($R=218.7\chi_0/\gamma\mu_{eff}^2$, χ_0 is in units of 10^{-3} emu/mol and γ in mJ/mol K^2) about 2, whereas $CeInPt_4$ has a Wilson ratio=0.64, using μ_{eff} $=1.29$ μ_B, $\gamma=2.5$ J/mol K^2, and $\chi_0=12.1\times 10^{-3}$ emu/mol. The Wilson ratio has been shown to be 2 for a spin-1/2 Kondo system.[27] The value of R shows that the Kondo effect prevents the high temperature moment (from Curie-Weiss) undergoing long range order at low temperatures. The trend in R suggests that the systems vary from magnetic (R

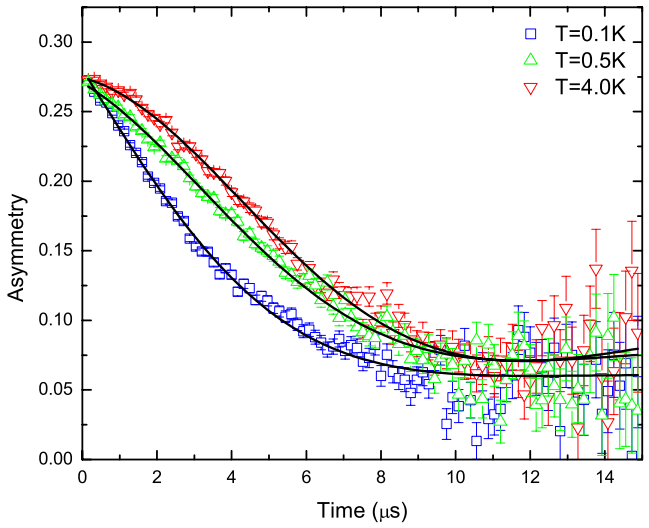

FIG. 5. (Color online) The μSR spectra from $CeInPt_4$ collected at 0.1 K (□), 0.5 K (△), and 4.0 K (▽) in zero field. The lines are a least-squares fit to the data using Eq. (3).

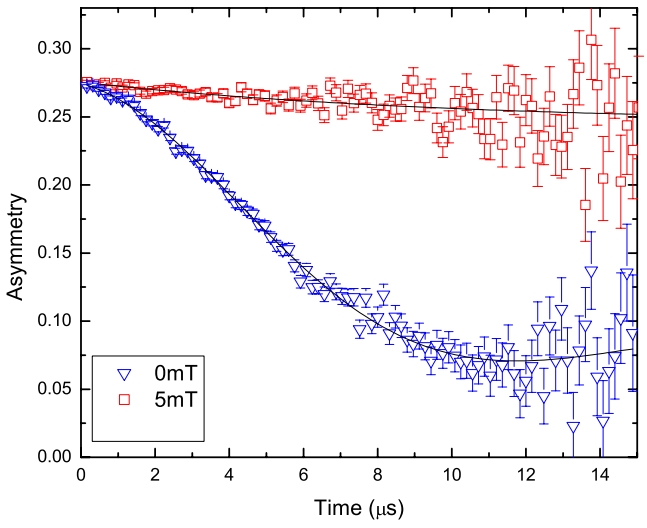

FIG. 6. (Color online) μSR spectra from $CeInPt_4$ collected at 4 K in zero field (▽) and with a longitudinal field of 5 mT (□). The lines are the least-squares fit to the data using Eqs. (3) and (4) for the zero field and the applied field data, respectively.

$=0.8-2.1$) to nonmagnetic ($R=0.56-0.75$) to superconducting ($R<0.52$). This suggests that $CeInPt_4$ should be nonmagnetic as indeed is the case.[28]

V. MUON SPIN RELAXATION MEASUREMENTS

The zero field μSR spectra were fitted using a static Gaussian Kubo-Toyabe function multiplied by an exponential decay with constant background A_{bckgrd},

$$G_z(t) = A_0\left[\frac{1}{3} + \frac{2}{3}(1-\sigma^2t^2)\exp\left(-\frac{\sigma^2t^2}{2}\right)\right]\exp(-\lambda t) + A_{bckgrd}, \tag{3}$$

where A_0 is the initial asymmetry, σ is the nuclear contribution, and λ is the electronic relaxation rate. The static Gaussian Kubo-Toyabe function results from a Gaussian distribution of local magnetic fields at the muon site which arise from the nuclear spins.[29] The exponential decay, $\exp(-\lambda t)$, is the magnetic contribution which results from the dynamic magnetic fields which arise from the fluctuating atomic spins. The multiplicative nature of the nuclear and magnetic contributions is only valid if these processes are independent. For $CeInPt_4$, this is clearly the case. Typical zero field μSR spectra obtained from $CeInPt_4$ are shown in Fig. 5, together with a least-squares fit to the data using Eq. (3).

The nuclear contribution to Eq. (3) gives direct information on the muon site, while the magnetic contribution gives information on the spin dynamics of $CeInPt_4$. In some systems, it is possible to decouple the nuclear contribution from the electronic contribution by applying a small longitudinal field. This is the case for $CeInPt_4$ where the application of a 5 mT longitudinal field is enough to decouple the nuclear component (see Fig. 6). Once the nuclear component has been decoupled, the spectra are best described by

$$G_z(t) = A_0\exp(-\lambda t) + A_{bckgrd}. \tag{4}$$

However, if the applied longitudinal field is increased still further, then it is possible to decouple the electronic moments. Using this information, we can obtain the internal field width at the muon site and the correlation time. We shall now discuss all these contributions in turn.

A. Nuclear contribution and the determination of the muon site in $CeInPt_4$

The nuclear contribution in Eq. (3) is the Gaussian Kubo-Toyabe function. In deriving the Kubo-Toyabe function, it is assumed that the muons are stationary (i.e., no hopping within the lattice) and that the three orthogonal components of the magnetic field have a Gaussian distribution centered around zero with a width Δ.[29] The nuclear depolarization rate σ is related to Δ by

$$\sigma^2 = \gamma_\mu^2\Delta^2, \tag{5}$$

where γ_μ is the gyromagnetic ratio of the muon (=13.55 kHz/G). Figure 5 shows the zero field data for a range of temperatures. The fits to the data show that A_0, σ, and A_{bckgrd} are temperature independent and that the nuclear depolarization rate σ is 0.147 μs^{-1}. The lack of temperature dependence in σ indicates that the muons are static within the lattice at temperatures below 4 K. Using finite element analysis, σ has been determined over a $4\times4\times4$ unit cell, in order to reduce end effects, using the relation[30]

$$\sigma^2 = \frac{1}{6}I(I+1)\frac{8}{3}\left(\frac{\mu_0\hbar}{4\pi}\gamma_\mu\gamma_n\right)^2\left(1+\frac{3}{8}\frac{I+\frac{1}{2}}{I(I+1)}\right)\sum_{i=1}^{N}\frac{1}{r_i^6}, \tag{6}$$

where I is the nuclear spin and γ_n is the gyromagnetic ratio of the nucleus. When this calculation is performed for $CeInPt_4$, the most probable muon site in the unit cell is found to be at $(\frac{1}{2},\frac{1}{2},\frac{1}{4})$ and equivalent sites (see Fig. 7). This site is a large interstitial void within the unit cell.

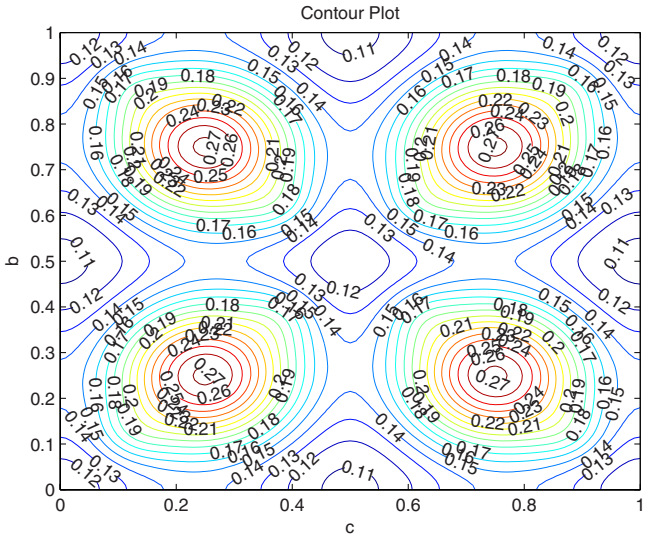

FIG. 7. (Color online) A contour plot of the muon depolarization rate for $x=0.5$ plane. The proposed muon sites are at $\left(\frac{1}{2},\frac{1}{2},\frac{1}{4}\right)$ and equivalent sites.

B. Spin dynamics in $CeInPt_4$

The muon spin relaxation function generally takes the form of an exponential decay as given in Eq. (4) for a system of noninteracting electronic spins, characterized by a unique spin relaxation rate. The exponential decay of the atomic muon spin relaxation corresponds to a simple exponential form of the time dependent autocorrelation function at the muon site. Moreover, the single exponential behavior shows that there is no evidence of any magnetic frustration. The λ is the electronic contribution to the relaxation rate and is related to the second moment of the atomic magnetic field distribution $\langle B\rangle^2$ and the correlation time τ_c by the relation

$$\lambda = \gamma_\mu^2 \langle B\rangle^2 \tau_c. \tag{7}$$

The temperature dependence of the magnetic depolarization rate will, therefore, vary as the internal field and the correlation time of the spin fluctuations change. Moreover, it has been shown λ is related directly to the local susceptibility,[31–33] χ_L,

$$\lambda = \frac{G k_B T \chi_L}{\Gamma}, \tag{8}$$

where χ_L is defined as

$$\chi_L = \frac{1}{N}\sum_q \chi(q), \tag{9}$$

G is the hyperfine coupling constant, and Γ is the linewidth. In general, this results in λ diverging as the temperature is reduced.

As previously mentioned, all the zero field μSR spectra are well described by Eq. (3) with A_0, σ, λ, and A_{bckgrd} as free parameters. The coefficients A_0, σ, and A_{bckgrd} are found to be temperature independent and, therefore, the contribution from the atomic fields is extremely motionally narrowed. We have not observed any oscillations or reduction in the value of A_0 as a function of temperature, which shows that no static magnetic order is present down to the lowest temperature. Indeed, the only parameter that shows a temperature dependence is λ (see Fig. 8), which diverges as $T \rightarrow 0$ K. Further, over the entire temperature range of the measurements, the temperature dependence of λ is shown to be of an Arrhenius-like behavior (see Fig. 8), i.e., follows the form

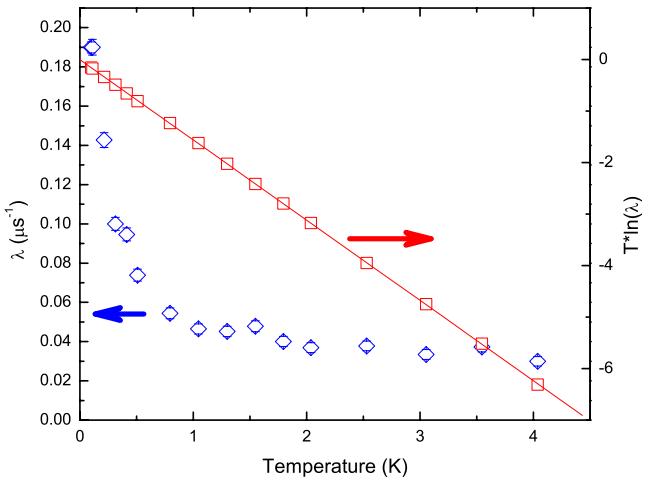

FIG. 8. (Color online) The temperature dependence of the electronic contribution λ of the muon depolarization (blue ◇). The red □ display the Arrhenius behavior of λ, and the line is a least-squares fit of Eq. (10) to the data.

$$\lambda = \lambda_0 \exp\left(-\frac{E_a}{kT}\right), \tag{10}$$

where E_a is an activation energy and k is the Boltzmann constant. This shows that the spin dynamics within $CeInPt_4$ is a thermally activated process with $E_a=2.9$ mK. Therefore, there are low energy spin fluctuations present in $CeInPt_4$.

Applying a longitudinal field which is large enough to decouple the electronic moments can yield information on the internal field width at the muon site and on the correlation time. Figure 9 shows the field dependence of λ at 45 mK, which reveals that λ decreases slowly with increasing field. This field effect on λ is well described by the conventional formula[31]

$$\lambda = \frac{2\Delta^2/\nu}{1+(\gamma_\mu B_{ext}/\nu)^2}, \tag{11}$$

where Δ^2/γ_μ^2 is the variance of the components of the field distribution at the muon site, ν is spin fluctuation rate, and B_{ext} is the applied magnetic field. The fit to the data gives $\nu=270(30)$ MHz and $\Delta=6.1(3)$ μs^{-1}; hence, $\Delta/\gamma_\mu \approx 71$ mT. Using these values and taking into account the position of the muon, we find that Ce ions are likely to have a reduced moment of ≈ 0.25 μ_B in $CeInPt_4$. This shows that Kondo screening is considerably reducing the $4f$ moment on the Ce ion.

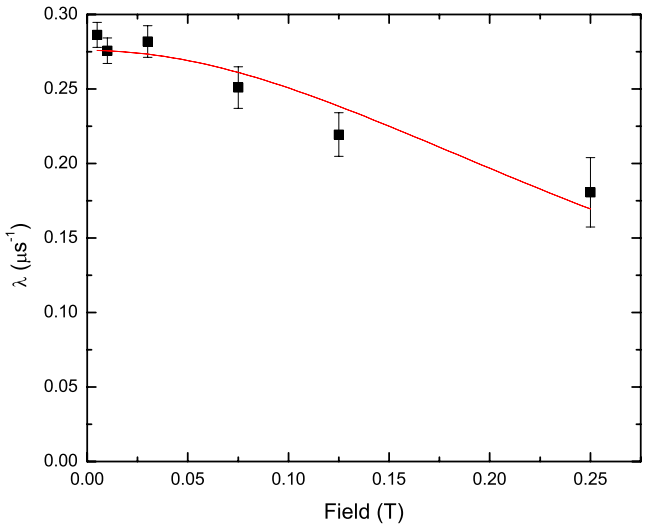

FIG. 9. (Color online) Field dependence of the electronic relaxation rate λ for $CeInPt_4$ at 45 mK. The line is a least-squares fit of Eq. (11) to the data.

VI. INELASTIC NEUTRON SCATTERING

Figure 10 shows the observed scattering from the low angle bank (red-filled down triangles) at 19°, at a distance of 2.5 m, and estimated phonon contribution scaled from the high angle bank at 135°, at a distance of 4 m, at 13 K (blue-filled up triangles). Extra magnetic scattering centered at 25 meV at low angle is clearly visible, which is attributed to the crystal field excitation of the Ce^{3+} ion on a site with cubic point symmetry.[34] The cubic point symmetry of the Ce ions in $CeInPt_4$ gives only one independent crystal field parameter in the crystal field Hamiltonian,

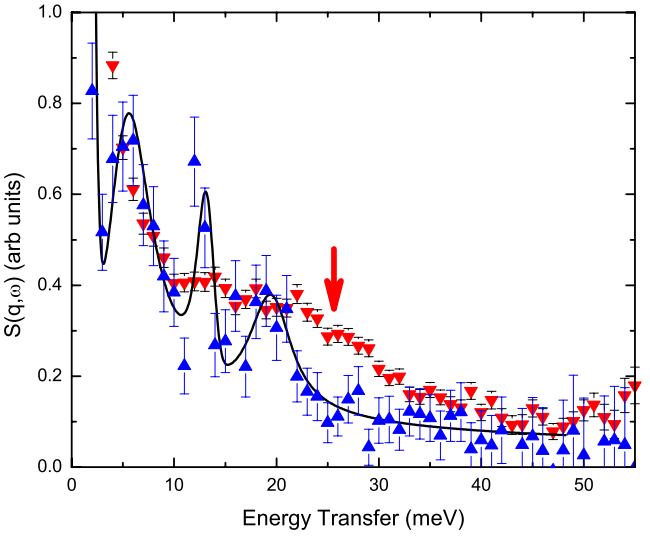

FIG. 10. (Color online) INS spectra from $CeInPt_4$ at 13 K. The red ▽ symbols show the total INS scattering (both magnetic and phonon); the blue △ symbols show the estimated phonons from the high angle bank. The solid line is a fit to the phonon scattering using a Lorentzian function. The arrow indicates the region of additional magnetic scattering which exhibits a crystal field excitation at ~25 meV.

$$H_{CF} = B_4^0(O_4^0 + 5O_4^4), \tag{12}$$

where B_4^0 is the crystal field parameter and O_n^m are the Stevens operators.[35] Under the cubic crystal field potential, the $J=5/2$ multiplet of the Ce^{3+} ions splits into a doublet (Γ_7) and a quartet (Γ_8), with energy eigenvalues of $-240B_4^0$ and $120B_4^0$, respectively, which gives one inelastic excitation. Thus, inelastic neutron scattering is a direct method of estimating the crystal field (CF) parameter from the measured position of the inelastic excitation, $\Delta_{CF}=360B_4^0$. However, from the peak position only, it is not possible to determine the sign of B_4^0, i.e., to decide whether the crystal field ground state is a doublet Γ_7 or a quartet Γ_8. In order to determine the ground state, one needs to compare the observed intensities of the quasielastic and inelastic peaks and also their temperature dependences with those calculated on the basis of the crystal field model.[36] The present data give a value of $B_4^0 = 0.069$ meV, but it was not possible to conclude on the nature of the ground state of the Ce ion in $CeInPt_4$ from the inelastic neutron scattering (INS) data alone. To check the ground state of $CeInPt_4$ and the sign of B_4^0 (+ sign indicates Γ_7 as a ground state and − sign indicates Γ_8 as a ground state), we calculated the susceptibility for both Γ_7 and Γ_8 as the ground states. Our present calculations clearly show that the ground state is a doublet, which is in agreement with the previous study.[9] It is interesting to note that despite $CeInPt_4$ having a crystallographically ordered structure, the linewidth of crystal field excitation is very large >10 meV. The origin of the large width can be attributed to the hybridization between the $4f$ and the conduction electrons. Furthermore, it is interesting to note that the phonon scattering observed in Fig. 10 reveals a clear peak at 5 meV. This low energy phonon peak is attributed to a rattling mode of the In atoms. This has also been observed in other systems.[37]

VII. CONCLUSIONS

Our neutron diffraction study shows that $CeInPt_4$ crystallizes into a $F\bar{4}3m$-type structure. There is no evidence for a deviation from complete order of In and Pt on crystallographic $4c$ and $16e$ sites. The In atoms exhibit a large atomic displacement parameter, which is attributed to a rattling mode which is confirmed by the observation of a 5 meV phonon peak in our inelastic neutron scattering. The heat capacity shows a remarkable high value of the electronic specific heat coefficient (2.5 $J/mol\,K^2$) and does not show any evidence of magnetic order. The logarithmic temperature dependence of C/T indicates that $CeInPt_4$ exhibits non-Fermi-liquid behavior close to a $T=0$ quantum critical point. μSR measurements show no evidence of any magnetic frustration or indeed magnetic order for $T>40$ mK, but rather the presence of low energy spin fluctuations that suppress any magnetic order, which is responsible for the high γ value. The inelastic neutron scattering results together with the magnetization measurements reveal that the crystal field ground state of the Ce^{3+} is a Γ_7 doublet. Further, the observed large width of the crystal field excitation, along with a large reduction in the estimated moment from the μSR measurements, suggests the presence of strong hybridization be-

tween the Ce $4f$ electrons and the conduction band, which is consistent with the high value of the Curie-Weiss temperature (−255 K) observed in the magnetization measurements. The comparison of residual resistivity and observed normalized muon relaxation rate at the lowest temperature[38] of $CeInPt_4$ suggests that the disorder is playing minor role in $CeInPt_4$ compared with that in $UCu_{3.5}Pd_{1.5}$ and much smaller compared with UCu_4Pd. One cannot avoid that some role is played by the disorder in the origin of NFL of $CeInPt_4$, but the low value of $T_K=2$ K suggests that the physics is dominated by the $T=0$ K quantum fluctuations as supported through the temperature dependence of the heat capacity and the low energy spin fluctuations observed in our μSR study.

ACKNOWLEDGMENTS

We would like to thank Herwig Michor for fruitful discussion and Ian Terry for access to the low temperature SQUID at Durham University.

[1] G. R. Stewart, Rev. Mod. Phys. **73**, 797 (2001).
[2] P. Coleman, arXiv:cond-mat/0612006 (unpublished).
[3] H. Tsunetsugu, M. Sigrist, and K. Ueda, Rev. Mod. Phys. **69**, 809 (1997).
[4] L. Degiorgi, Rev. Mod. Phys. **71**, 687 (1999).
[5] S. K. Dhar, S. K. Malik, and R. Vijayaraghavan, J. Phys. C **14**, L321 (1981).
[6] S. K. Malik and D. T. Adroja, Phys. Rev. B **43**, 6277 (1991).
[7] I. Felner and I. Nowik, Phys. Rev. B **33**, 617 (1986).
[8] A. P. Pikul, D. Kaczorowski, Z. Bukowski, K. Gofryk, U. Burkhardt, Yu. Grin, and F. Steglich, Phys. Rev. B **73**, 092406 (2006).
[9] S. K. Malik, D. T. Adroja, M. Slaski, B. D. Dunlap, and A. Umezawa, Phys. Rev. B **40**, 9378 (1989).
[10] V. Fritsch, J. D. Thompson, and J. L. Sarrao, Phys. Rev. B **71**, 132401 (2005).
[11] H. Nakamura, K. Ito, and M. Shiga, J. Phys.: Condens. Matter **6**, 9201 (1994).
[12] I. I. Mazin, Phys. Rev. B **73**, 012415 (2006).
[13] T. Takeshita, S. K. Malik, and W. E. Wallace, J. Solid State Chem. **23**, 225 (1977).
[14] D. Read, I. Terry, and S. R. Giblin, Rev. Sci. Instrum. **77**, 103906 (2006).
[15] D. T. Adroja, J.-G. Park, E. A. Goremychkin, K. A. McEwen, N. Takeda, B. D. Rainford, K. S. Knight, J. W. Taylor, J. Park, H. C. Walker, R. Osborn, and P. S. Riseborough, Phys. Rev. B **75**, 014418 (2007).
[16] R. Chau, M. B. Maple, and R. A. Robinson, Phys. Rev. B **58**, 139 (1998).
[17] T. Sasakawa, K. Shigetoh, D. Hirata, K. Umeo, and T. Takabatake, Physica B **359-361**, 111 (2005).
[18] U. Killer, E.-W. Scheidt, G. Eickerling, H. Michor, J. Sereni, Th. Pruschke, and S. Kehrein, Phys. Rev. Lett. **93**, 216404 (2004).
[19] A. P. Pikul, N. Caroca-Canales, M. Deppe, P. Gegenwart, J. G. Sereni, C. Geibel, and F. Steglich, J. Phys.: Condens. Matter **18**, L535 (2006).
[20] A. Schroder, R. Van derBreg, H. V. Lohneysen, W. Paul, and H. Luken, Solid State Commun. **65**, 99 (1988).
[21] E. Sagmeister, E. Bauer, E. Gratz, H. Michor, and G. Hilscher, Physica B **230-232**, 148 (1997).
[22] D. T. Adroja, S. K. Malik, B. D. Padalia, and R. Vijayaraghavan, Solid State Commun. **71**, 649 (1989).
[23] Q. Si, S. Rabello, K. Ingersent, and J. Lleweilun Smith, Nature (London) **413**, 804 (2001).
[24] P. Coleman, C. Pepin, Q. Si, and R Ramazashvili, J. Phys.: Condens. Matter **13**, R723 (2001).
[25] P. Coleman, Physica B **259-261**, 353 (1999).
[26] A. Schroder, G. Aeppli, R. Coldea, M. Adams, O. Stockert, H. v. Löhneysen, E. Bucher, R. Ramazashvili, and P. Coleman, Nature (London) **407**, 351 (2000).
[27] K. G. Wilson, Rev. Mod. Phys. **47**, 773 (1975).
[28] G. R. Stewart, Rev. Mod. Phys. **56**, 755 (1984).
[29] R. S. Hayano, Y. J. Uemura, J. Imazato, N. Nishida, T. Yamazaki, and R. Kubo, Phys. Rev. B **20**, 850 (1979).
[30] A. Schenck, *Muon Spin Rotation* (Hilger, Bristol, 1985).
[31] A. Amato, Rev. Mod. Phys. **69**, 1119 (1997).
[32] B. D. Rainford, S. J. Dakin, and R. Cywinski, J. Magn. Magn. Mater. **104-107**, 805 (1992).
[33] B. D. Rainford, R. Cywinski, and S. J. Dakin, J. Magn. Magn. Mater. **140-144**, 805 (1995).
[34] Due to the difference in the instrument resolution of the 2.5 and 4 m detector banks, we are unable to extract the magnetic scattering by taking the difference of the two spectra in Fig. 10. It should also be noted that during these measurements, HET did not have the 2.5 m high angle bank.
[35] K. W. H. Stevens, Proc. Phys. Soc., London, Sect. A **65**, 209 (1952).
[36] M. T. Hutchings, *Solid State Physics* (Academic, New York, 1964), Vol. 16, p. 227.
[37] V. Keppens, D. Mandrus, B. C. Sales, B. C. Chakoumakos, P. Dai, R. Coldea, M. B. Maple, D. A. Gajewski, E. J. Freeman, and S. Bennington, Nature (London) **395**, 876 (1998).
[38] D. E. MacLaughlin, R. H. Heffner, O. O. Bernal, K. Ishida, J. E. Sonier, G. J. Nieuwenhuys, M. B. Maple, and G. R. Stewart, J. Phys.: Condens. Matter **16**, S4479 (2004).